Available online at www.sciencedirect.com
SCIENCE DIRECT
Polymer 47 (2006) 3946–3953
polymer
www.elsevier.com/locate/polymer

Dual lamellar crystal structure in poly(vinylidene fluoride)/acrylic rubber blends and its biaxial orientation behavior

Yongjin Li [a,*], Yuko Oono [a], Kazuo Nakayama [a], Hiroshi Shimizu [a], Takashi Inoue [b]

[a] *Nanotechnology Research Institute, National Institute of Advanced Industrial Science and Technology (AIST), Tsukuba Central 5, 1-1-1 Higashi, Tsukuba, Ibaraki 305-8565, Japan*
[b] *Department of Polymer Science and Engineering, Yamagata University, Yonezawa 992-8510, Japan*

Received 15 October 2005; received in revised form 24 February 2006; accepted 18 March 2006
Available online 18 April 2006

Abstract

The miscibility for melt-mixed poly(vinylidene fluoride) (PVDF)/acrylic rubber (ACM) blends and the crystal morphology of PVDF in the blends were investigated over the whole composition ranges by dynamic mechanical analysis (DMA), wide-angle X-ray diffraction (WAXD), small-angle X-ray scattering (SAXS), and transmission electron microscopy (TEM). DMA measurements revealed that PVDF is miscible with ACM in ACM-rich system, and partially miscible in PVDF-rich system. Two kinds of PVDF lamellar structures with different long periods were detected by SAXS and TEM for the partially miscible blends. In the miscible system, only one kind of crystal lamellae with enlarged long period is found. The two kinds of lamellar structures in the blend show different orientation behavior during the uniaxial stretching to result in a biaxial orientation. The lamellae with short long period are oriented vertical to the stretching direction, while those with large long period were found to be oriented parallel to the stretching direction.

Keywords: Blend; Miscibility; Crystal lamellae

1. Introduction

Polymer blends containing crystallizable components have received significant attentions because of the rich morphology offered by these systems. For a melt miscible crystalline/amorphous blend, three types of crystalline morphology can be created depending upon the location of molecular chains of amorphous component [1–3]: (1) interlamellar structure, where the molecular chains of the amorphous component are inserted into the lamellar gallery of the crystalline component; (2) interfibrillar structure, where the molecular chains of amorphous components are located in the region between the lamellar bundles in the spherulites; (3) interspherulic structure, where the amorphous constituent is expelled out of the spherulites. A blend system does not necessarily exhibit only one type of lamellar structure. Different morphological patterns can coexist in one system owing to multiple locations of the amorphous components [4,5].

Poly(vinylidene fluoride) (PVDF) is a highly crystalline polymer that is miscible with many polymers containing carbonyl group, such as polyacrylates [6–8], polyacetates [9,10], and polyketone [11], through the specific interactions of CF_2 dipoles with carbonyl group. The miscibility of PVDF with poly(methyl methacrylate) (PMMA) have been widely investigated in the literature, with analysis ranging from melting point depressions [12,13], changes in glass transition temperatures [14], phase diagrams [15,16], measurements of spherulite growth and crystallization rates [17], as well as lamellar structure [18]. The results indicate that the blend components are miscible in the melt and in the amorphous phase. PVDF crystallinity decreases progressively with increasing PMMA amount and only amorphous blend can be obtained with PMMA content more than 50%. For the semicrystalline blend, PMMA molecular chains are mainly incorporated between the PVDF lamellae. Both long period and amorphous layer thickness increase gradually with increasing PMMA content.

Acrylic rubber, ACM, is a copolymer of alkyl methacrylate, ethylene, and glycidyl methacrylate with about 40–60% alkyl methacrylate. It is expected that the specific interaction occurs for CF_2 group of PVDF and carbonyl group of ACM same to

* Corresponding author. Tel.: +81 29 861 4197; fax: 81 29 861 6294.
E-mail address: yongjin-li@aist.go.jp (Y. Li).

0032-3861/$ - see front matter © 2006 Elsevier Ltd. All rights reserved.
doi:10.1016/j.polymer.2006.03.075

that for PVDF and PMMA, but the interaction is weaker than that between PVDF and PMMA due to the lower carbonyl group concentration of the copolymer. Moreover, the flexible molecular chains of ACM may show less influence on the crystallization of PVDF because of its relatively low glass transition temperature (−13 °C), comparing to 110 °C of PMMA. Therefore, it is a great interest to investigate the PVDF crystallization behavior by the addition of ACM. Furthermore, the blending of PVDF and ACM will lead to a new oil and heat resistant thermoplastic elastomer by the dynamic vulcanization process [19]. In this work, blends of PVDF and ACM were prepared over the whole composition range by melt mixing. The miscibility between PVDF and ACM, crystal morphology and orientation behaviors of PVDF in the blend are investigated. Two constituent lamellae, with the long period of 22.5 and 12.6 nm, respectively, are observed in this crystalline/amorphous blend system when PVDF content is more than 60 wt%. It was further found that the two kinds of lamellae show different orientation behaviors by the uniaxially stretching. The lamellae with larger long period are oriented to be parallel to the stretching direction, while those with shorter long period are oriented to be vertical to the stretching direction.

2. Experimental section

2.1. Materials and sample preparation

PVDF and ACM samples used in this work were purchased from Kureha Chemicals and Nippon Zeon Co. Ltd, respectively. All the polymers were dried in a vacuum oven at 80 °C for at least 12 h before processing. The blends with various compositions were prepared using a Brabender-type plastic mixer (Toyoseiki Co. KF70V) with a two-rotors at a rotation speed of 100 rpm at 190 °C for 10 min. After blending, all the samples were then hot pressed at 200 °C to a film with a thickness of 500 μm, followed by quenching in ice water. The obtained films were used for the following characterization. Oriented samples were prepared by uniaxial stretching of the molded film to a draw ratio of four at 80 °C with a stretching speed of 20 mm/min. For the samples with the ACM content more than 70 wt%, the stretched samples under strain (by fixing the two ends of samples) were used for the X-ray measuring to prevent the relaxation of the samples during measurements.

2.2. Characterization

Dynamic mechanical analysis (DMA) was carried out with RHEOVIBRON DDV-25FP (Orientec Corp.) in a tensile mode. The dynamic storage and loss moduli were determined at a frequency of 1 Hz and a heating rate of 3 °C/min as a function of temperature from −150 to 170 °C.

Small-angle X-ray scattering (SAXS) patterns were obtained by microfocused Cu Kα radiation (45 kV, 60 mA) generated by an X-ray diffractometer (Rigaku Ultrax 4153A 172B) and an imaging plate detector. The exposure time was 6 h for each measurement.

Phase structure of the blends and crystal morphology of PVDF in the blends were observed directly using a transmission electron microscopy (TEM) (Hitachi H7000) operating at an acceleration voltage of 75 kV. The blend samples were ultra-microtomed at −120 °C to a section with a thickness of about 70 nm. The sections were then stained by ruthenium tetroxide (RuO_4) for 20 min.

Wide-angle X-ray diffraction (WAXD) profiles were obtained using Cu Kα radiation (40 kV, 120 mA) generated by an X-ray diffractometer (Rigaku, Ultrax 8000) with the scanning speed of 1°/min. WAXD patterns for the stretched samples were obtained by the same X-ray diffractometer with an imaging plate detector.

Differential scanning calorimetry (DSC) was carried out under nitrogen flow at a heating or cooling rate of 10 K/min with a Perkin–Elmer DSC-7 differential scanning calorimeter calibrated with the melting temperature of indium and zinc.

3. Results

3.1. Miscibility

It is well known that a single glass transition temperature (T_g) appears if the two components are miscible in the amorphous phase. The immiscibility will be demonstrated by appearance of the T_gs of both individual components. If two components are partially miscible, their T_gs would shift toward each other.

The dynamic loss in dynamic mechanical analysis, tan δ, is shown in Fig. 1 as a function of temperature for the neat components and the blends. The peak temperature of tan δ is used to denote the T_g. For the blends with less than 60 wt% PVDF, only one T_g can be detected, indicating the miscible state between ACM and the amorphous part of PVDF. In contrast, the two components are partially miscible when PVDF is more than 60 wt% because two shifted T_gs are observed, as shown in Fig. 2. The fact that two T_gs are observed reveals that two-phase structure for the blends when PVDF content is more than 60 wt%. It is considered that the two phases are PVDF rich phase and ACM rich phase, respectively. It should be noted that the PVDF molecules in ACM rich phase are crystallizable even though the concentration of PVDF in the phase is relatively low.

Assuming simply 50% crystallinity of PVDF, the T_g curve was calculated by the Fox equation [20]. The result is displayed in Fig. 2. The calculated curve(-●-) is not far from the observed curve (-■-).

3.2. Lamellar structure and crystal forms

Fig. 3 displays the Lorentz-corrected SAXS profiles of pure PVDF and PVDF/ACM blends. The SAXS intensity was normalized by thickness and exposure time, after subtracting air scattering from the observed profiles. It shows that PVDF exhibits a scattering peak at $q = 0.57\ nm^{-1}$, corresponding to

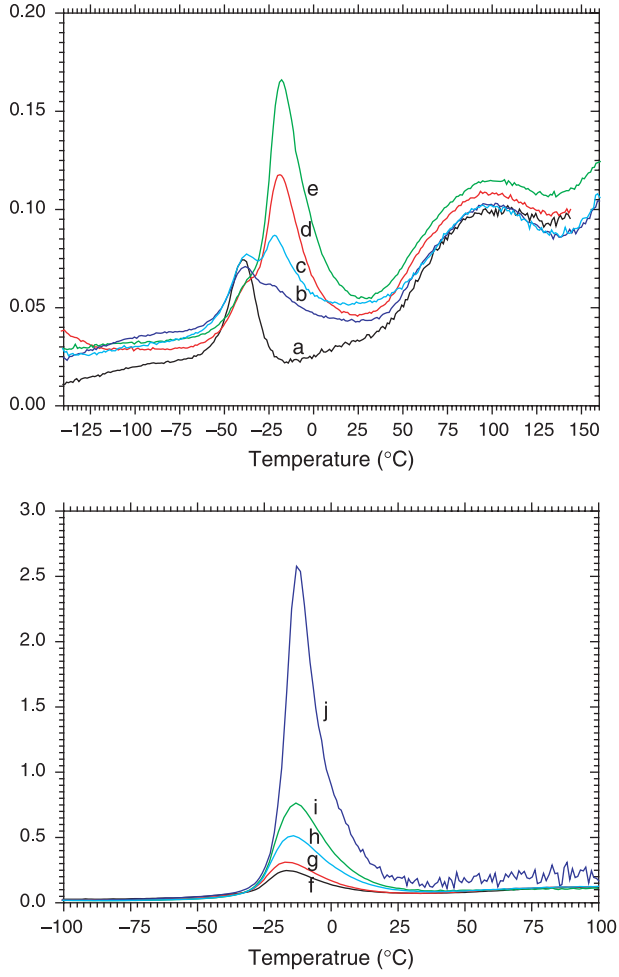

Fig. 1. tan δ versus temperature for the PVDF/ACM blends with various composition ratios: (a) neat PVDF, (b) PVDF/ACM=95/5, (c) PVDF/ACM=90/10, (d) PVDF/ACM=80/20, (e) PVDF/ACM=70/30, (f) PVDF/ACM=60/40, (g) PVDF/ACM=50/50, (h) PVDF/ACM=40/60, (i) PVDF/ACM=20/80, (j) neat ACM.

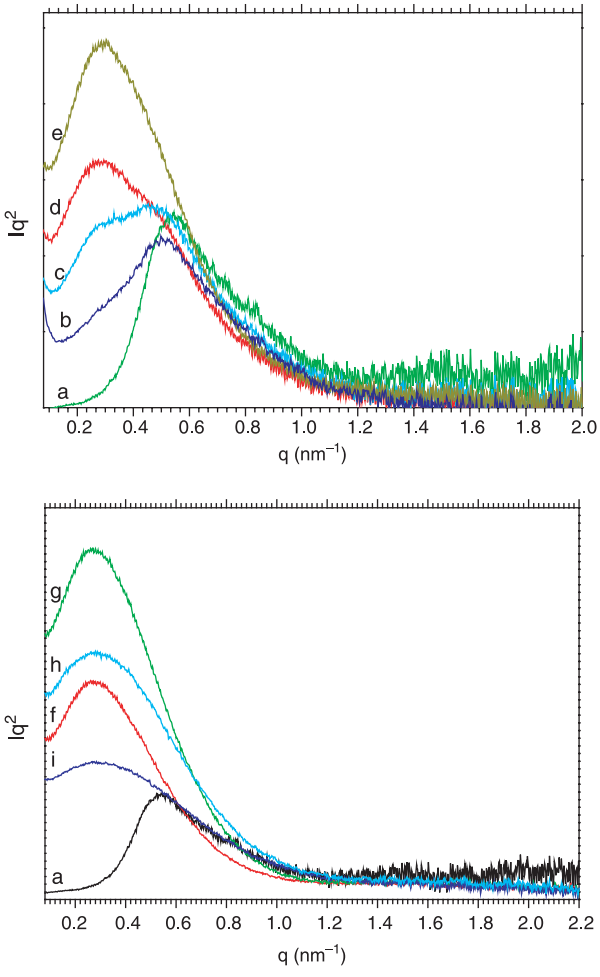

Fig. 3. Lorentz-corrected SAXS profiles for the PVDF/ACM blends: (a) neat PVDF, (b) PVDF/ACM=95/5, (c) PVDF/ACM=90/10, (d) PVDF/ACM=80/20, (e) PVDF/ACM=70/30, (f) PVDF/ACM=60/40, (g) PVDF/ACM=40/60, (h) PVDF/ACM=20/80, (i) PVDF/ACM=10/90.

the crystal long period of $L=11$ nm. On the other hand, the PVDF/ACM blends with more than 60 wt% PVDF show two scattering peaks at $q=0.5\ \mathrm{nm}^{-1}$ ($L=12.56$ nm) and $q=0.28\ \mathrm{nm}^{-1}$ ($L=22.4$ nm), indicating that two kinds of

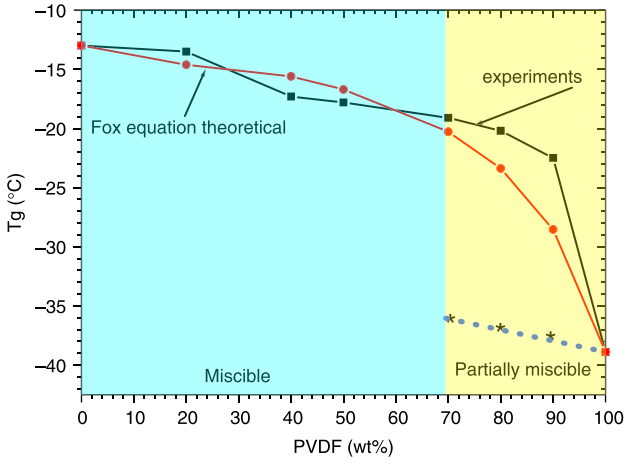

Fig. 2. Glass transition temperature of PVDF/ACM blends.

crystal lamellae coexist in one system. Dual lamellar structure has been observed for many crystalline homopolymers. During crystallization, primary lamellar stacks are formed first comprising thicker crystalline lamellae, whereas secondary lamellar stacks are formed later between the primary lamellar stacks [21–24]. For the present case, however, the two lamellar constituents may originate from the partially miscible nature of the blends, which is also confirmed by the TEM observations (see the following part). The crystals with large long period of 22.4 nm (designated at the LLP crystals hereafter) come from the PVDF crystals in the ACM rich phase, in which many ACM molecular chains are incorporated into the gallery of PVDF to form the interlamellar structure. In contrast, the crystals with short long period of 12.5 nm (designated as SLP crystals hereafter) are the crystals in the PVDF rich phase. These crystals have only a slightly increased long period as compared with those in neat PVDF. With increasing the ACM contents in the blends, the intensity of the scattering peak at $q=0.28\ \mathrm{nm}^{-1}$ increases progressively, indicating the gradually increment of LLP crystal content.

For the samples with PVDF content less than 60 wt%, only one scattering peak at $q=0.26\ \mathrm{nm}^{-1}$ ($L=24.1$ nm) can be observed from the SAXS Lorentz-corrected profiles, indicating the uniform crystal lamellae (LLP crystals) in the ACM rich blends. The enlarged long period and the scattering intensity enhancement comparing to the neat PVDF can be attributed to the incorporation of ACM molecular chains in the regions between the individual PVDF lamellae. However, the scattering intensity decreases continuously with increasing the ACM content in the blend from 60 to 90% due to the decreasing of percentage of crystalline part in the blend system.

Fig. 4 shows the TEM micrographs of PVDF/ACM blends. For the PVDF/ACM 80/20 blend (Fig. 4(a)), two regions (designated to regions A and B) can be discerned. It is considered that the bright part is the PVDF-rich region with a small amount of ACM occluded inside because PVDF is hardly stained RuO_4. The scattering from short long period of about 12.5 nm in the SAXS profiles originates from the PVDF crystals in this region. On the other hand, the grey part in Fig. 4(a) is considered to be the ACM-rich region. In this region, PVDF crystal lamellae can be clearly observed and the long period of the observed lamellae is determined to be about 22 nm from the TEM photographs. Therefore, the scattering peak at $q=0.28\ \mathrm{nm}^{-1}$ in the SAXS profile (Fig. 3(a)) can be assigned to the PVDF lamellar spacing in this region. For the blends with PVDF less than 60 wt%, the two-region nature is not seen. PVDF lamellae with enlarged long period (LLP crystals) are precisely dispersed in the grey region. The typical TEM photograph is shown in Fig. 4(b) for the PVDF/ACM 10/90 sample.

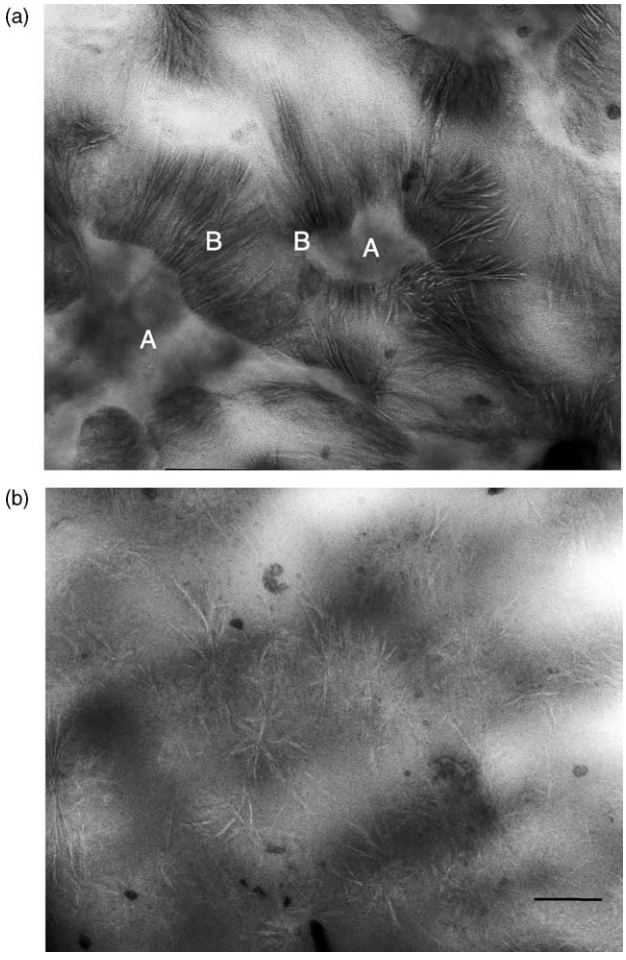

Fig. 4. TEM micrographs for (a) PVDF/ACM=80/20 (part A is designated the PVDF-rich region and part B is designated the ACM-rich region), (b) PVDF/ACM=10/90. The scale bar in the image corresponds to 200 nm.

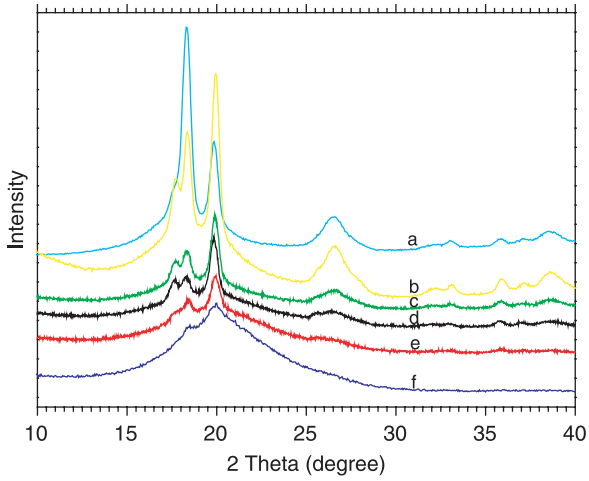

Fig. 5. WAXD profiles for (a) neat PVDF, (b) PVDF/ACM=80/20, (c) PVDF/ACM=60/40, (d) PVDF/ACM=40/60, (e) PVDF/ACM=20/80, (f) PVDF/ACM=10/90.

The WAXD profiles of neat PVDF and the blends are shown in Fig. 5. Both neat PVDF and all blends show the typical reflection patterns with the α crystal form of PVDF, indicating no crystal form transition occurs by the blending with ACM.

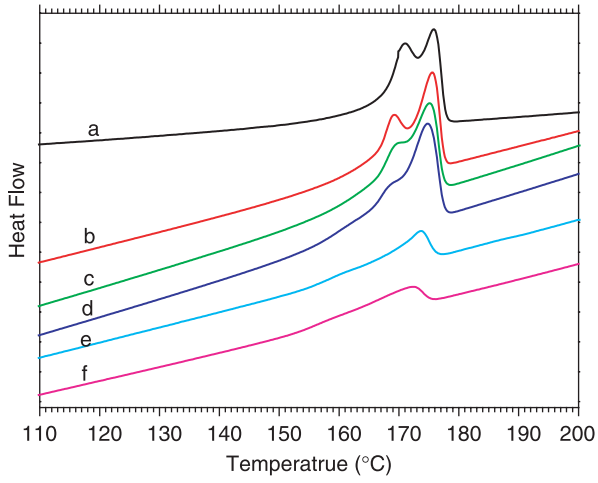

Fig. 6. DSC thermograms during heating for PVDF/ACM blends: (a) neat PVDF, (b) PVDF/ACM=80/20, (c) PVDF/ACM=60/40, (d) PVDF/ACM=40/60, (e) PVDF/ACM=20/80, (f) PVDF/ACM=10/90.

3.3. Thermal properties

Most of miscible polymer blends containing crystalline components show the melting point depression because of the thermodynamic interaction between the component polymers [25,26]. However, no marked decreasing in melting temperature over the whole composition range can be observed for the present blend system, as shown in the DSC curves during melting process in Fig. 6. The phenomena may be attributed to the relatively weak interactions between PVDF and ACM, as well as the very low glass transition temperature of ACM comparing to the crystallization temperature of PVDF.

3.4. Crystal orientation during stretching

Fig. 7 shows the WAXD patterns of drawn films of PVDF and the blends with various composition ratios stretched at 80 °C. The WAXD pattern of PVDF shows that α and β crystalline forms coexist in the oriented sample. The former exhibits the characteristic (100) and (020) reflections at $2\theta =$ 17.6 and 18.8°, respectively, on the equator, whereas the latter

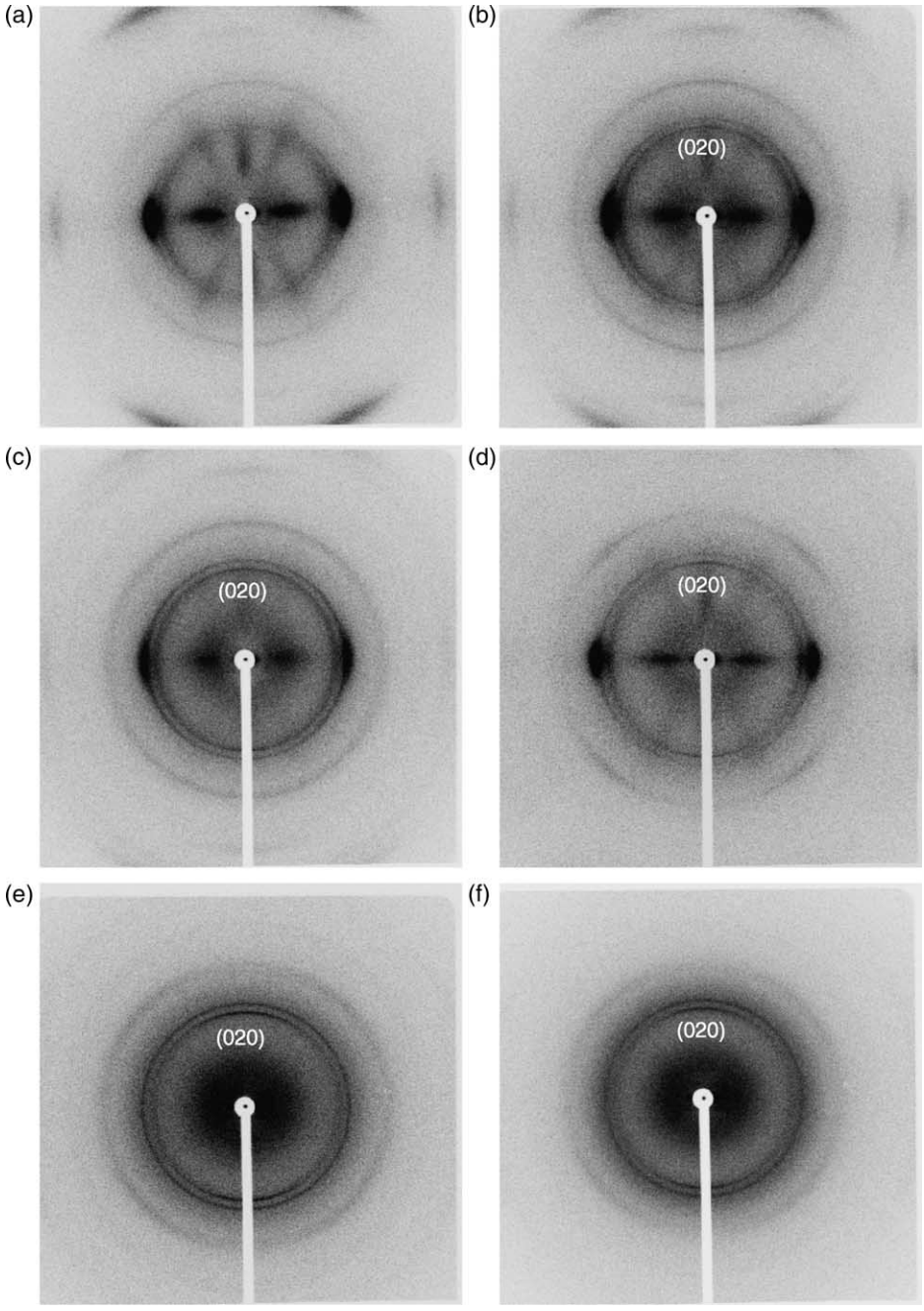

Fig. 7. WAXD patterns of the oriented PVDF/ACM blends with the draw ratio of four: (a) neat PVDF, (b) PVDF/ACM = 90/10, (c) PVDF/ACM = 80/20, (d) PVDF/ACM = 70/30, (e) PVDF/ACM = 50/50, (f) PVDF/ACM = 20/80.

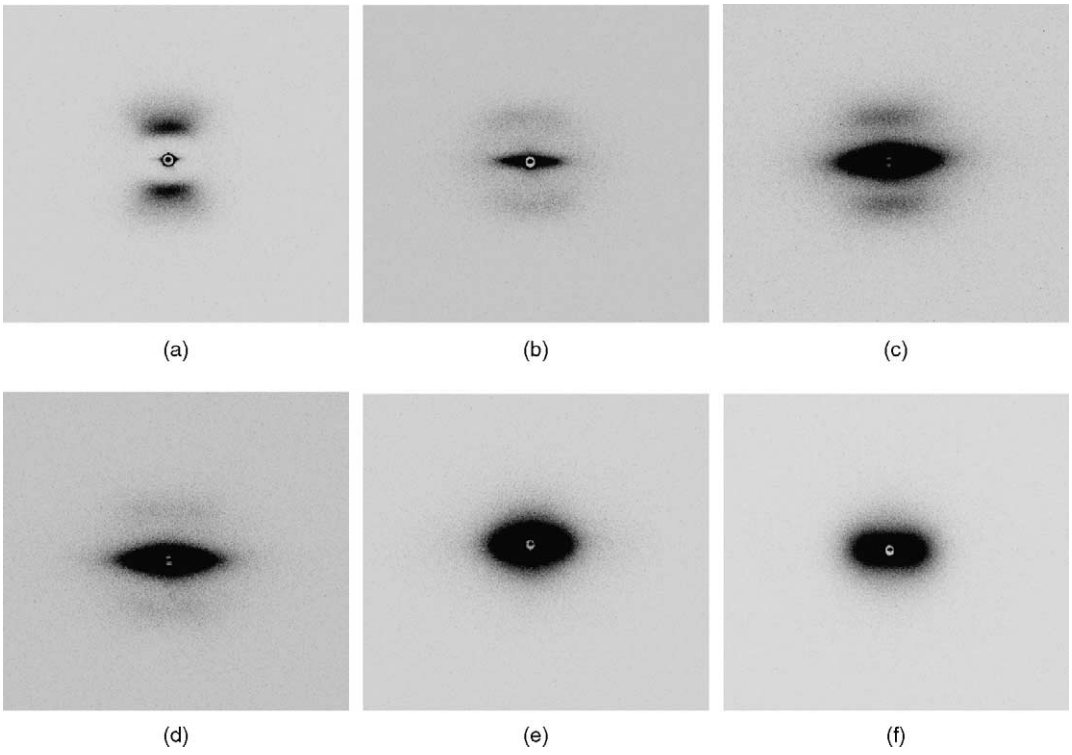

Fig. 8. SAXS patterns of the oriented PVDF/ACM blends with the draw ratio of four: (a) neat PVDF, (b) PVDF/ACM=95/5, (c) PVDF/ACM=80/20, (d) PVDF/ACM=70/30, (e) PVDF/ACM=50/50, (f) PVDF/ACM=20/80.

gives the (110)/(200) reflections at $2\theta = 20.5°$ on the equator. The fact that the (*hk*0) reflections of both α and β crystals are observed only on the equator reveals that the crystal lamellae of oriented PVDF are perpendicular to the stretching direction (*c*-axis oriented texture). For the PVDF/ACM 90/10 blend sample, however, a pair of weak reflection arcs at $2\theta = 18.8°$ ((020) reflection of α crystals) are observed on the meridian direction, in addition to the equator reflections as neat PVDF, indicating that some crystals are oriented with the *b*-axis along the stretching direction (the long axis of lamellae are parallel to the stretching direction). The reflection intensity of (100) reflection on the meridian increases with increasing the ACM contents, while that on the equator decreases accordingly. It means that the fraction of the *b*-axis oriented crystals is increased by increasing ACM content. For the blends with more than 40 wt% ACM, only *b*-axis oriented crystals can be observed, as shown in Fig. 7.

Fig. 8 shows the SAXS images for the stretched PVDF and PVDF/ACM blends. For the oriented neat PVDF, the scattering lobes are located only in the meridian direction, indicating that the lamellae are stacked along the stretching direction. For the oriented blends with more than 60 wt% PVDF, however, a very strong scattering can be observed in the equator direction in addition to the meridian lobes. In contrast, only the equatorial scattering is observed when the PVDF content is less than 60 wt%. The scattering in equatorial direction indicates the large electron density fluctuation is induced perpendicular to the stretch direction and that there exist some periodic structures perpendicular to the stretching direction.

By comparing the WAXD and SAXS patterns for the oriented samples, it can be concluded that the meridian scattering originates from the crystal lamellae stacked along the stretching direction, while that the equatorial strong scattering comes from the crystal lamellae stacked perpendicular to the stretching direction. Figs. 9 and 10 display the Lorentz-corrected SAXS profiles for the all stretched sample on the meridian and equatorial directions, respectively. The meridian profiles give the long period of about 11 nm and close

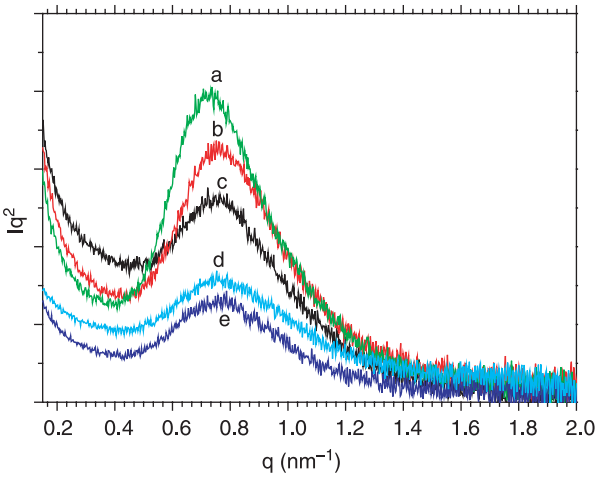

Fig. 9. Lorentz-corrected SAXS profiles of oriented samples in the meridional direction: (a) neat PVDF, (b) PVDF/ACM=95/5, (c) PVDF/ACM=90/10, (d) PVDF/ACM=80/20, (e) PVDF/ACM=70/30.

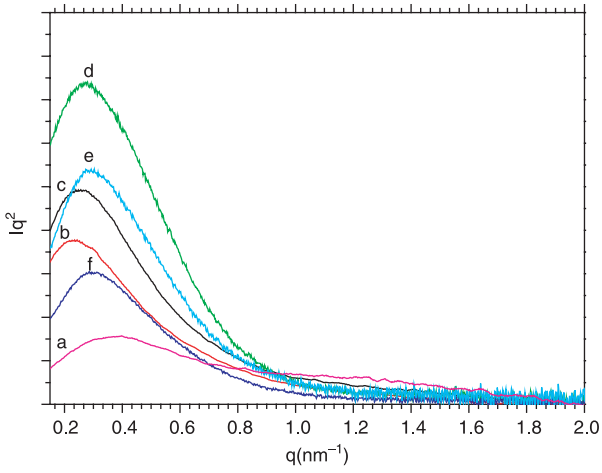

Fig. 10. Lorentz-corrected SAXS profiles of oriented samples in the equatorial direction: (a) PVDF/ACM=95/5, (b) PVDF/ACM=90/10, (c) PVDF/ACM=80/20, (d) PVDF/ACM=50/50, (e) PVDF/ACM=40/60, (f) PVDF/ACM=20/80.

to the values of the long period of SLP crystals. On the other hand, the equatorial SAXS profiles display apparent scattering peaks at $q=0.23\ \mathrm{nm}^{-1}$. The corresponding long period is almost same to that of the LLP crystals. In other words, the two kinds of lamellar structure for the PVDF/ACM blends in the isotropic state show different orientation behaviors during the uniaxially stretching. The *c*-axis of SLP crystals is aligned along the stretching direction, same to the behavior of neat PVDF, while the *b*-axis of LLP crystals is oriented along the stretching direction. The fraction of the two orientation textures is dependent upon the fraction of the two kinds of crystals, which is determined by the ACM content in the blends.

4. Discussion

As shown by Figs. 7–10, the PVDF crystals in the two regions show different orientation behaviors, especially for the *b*-axis orientation of LLP crystals during uniaxially stretching. In fact, we have found that the ACM/PVDF blend with *b*-axis orientation shows superior tensile recovery (elasticity). It is required for the high performance thermoplastic elastomer [19]. Although the different orientation modes have been reported for different components in crystalline/crystalline blends [27–29], the observation of biaxially oriented lamellar morphology formed by one component is the first time, to our knowledge. It is clear that the incorporation of ACM molecules in PVDF crystal lamellae takes the key role for the *b*-axis orientation of PVDF crystals in ACM-rich region because only normal *c*-axis orientation has been observed for the crystal in

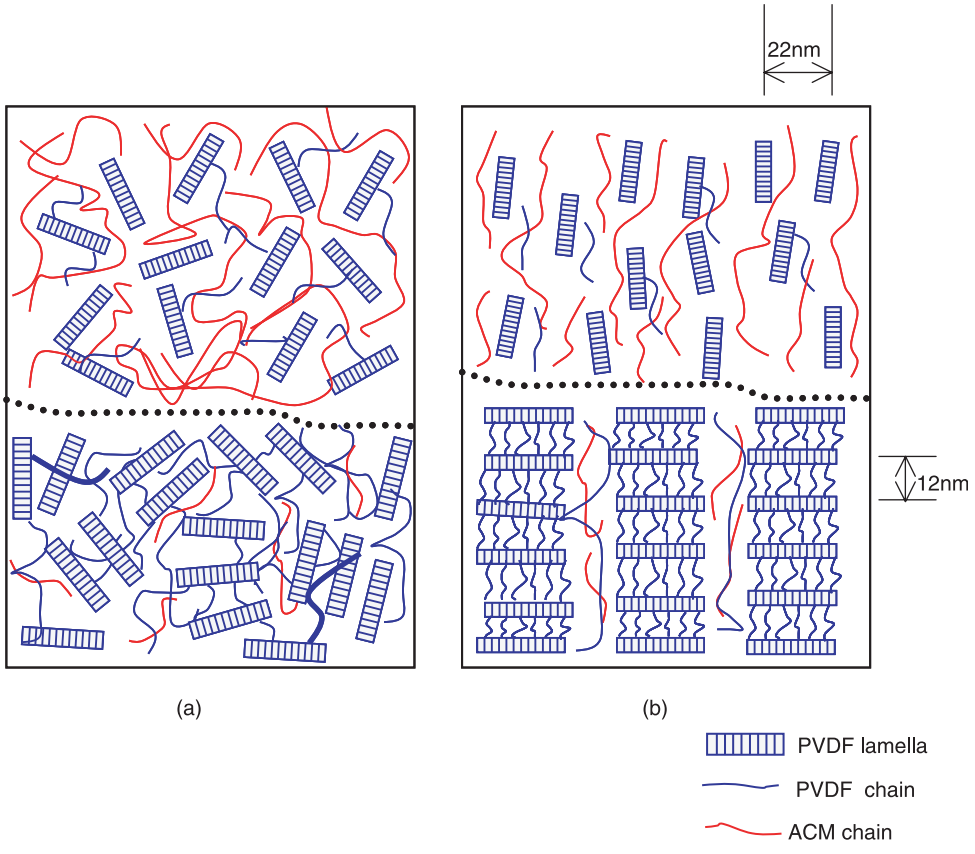

Fig. 11. Schematic illustration of the dual lamellar structure and the orientation behavior of PVDF crystals in the blends with ACM: (a) the dual lamellar structure for the PVDF/ACM partially miscible blends with more than 60 wt% PVDF, (b) the orientation behavior of the blends with the dual lamellar structure (the stretching direction is vertical).

PVDF-rich region and also in neat PVDF. The deformation process of semi-crystalline polymers has been extensively investigated [30]. Crystalline polymers consist of folded-chain lamellae joined by the amorphous part in the isotropic state. Many molecules in the amorphous part are trapped into the crystal lamellae and therefore as the tie-molecules to connect the different crystal lamellae. These tie-molecules will transform the stress from the amorphous part to the crystalline part during the stretching. Therefore, molecular chains (*c*-axis of lamellae) direction of crystalline polymer will be oriented along the drawing during stretching. The PVDF crystals in neat PVDF and the PVDF-rich region will follow this stretching mechanism. However, for the PVDF crystals in ACM-rich region and those in the blend with ACM content more than 40 wt%, the large amount of ACM molecule chains are inserted into the gallery of the PVDF lamellae, as shown in the schematic diagram of Fig. 11. PVDF forms very loose and sparse crystal lamellae, as shown in the SAXS and TEM results. Probably due to the diluent and impeding effects of ACM molecules, PVDF molecules hardly play a role of tie chains to connect the different crystal lamellae. In other words, the individual PVDF lamellae are isolated by the ACM molecules and simply dispersed in the ACM matrix. The isolated PVDF lamellae are like the long thin flat disk that embedded in the amorphous matrix. As the stretching proceeds, the ACM matrix is elongated along the stretching direction, and the PVDF crystal lamellae will be deformed and aligned with the long axis (*b*-axis) of the crystal lamellae along the stretching direction. Therefore, the PVDF crystal *c*-axis may be oriented perpendicular to the stretching direction, as shown in Fig. 11(b).

5. Conclusion

Crystal structure and orientation behavior of PVDF in its blend with ACM were studied over the whole component ratio. Two kinds of PVDF lamellae morphologies with different long periods are observed by the TEM and SAXS measurements for the partially miscible polymer blends where PVDF content is high than 60 wt%. When we stretch the partially miscible samples, the two kinds of lamellae show perpendicular orientation textures to form a biaxially oriented sample. The biaxially orientation of PVDF in one system is a new type of morphology of polymeric systems, in which the crystallites of the same polymer are oriented in mutually opposite direction. It is expected that this kind of biaxial orientation may lead to some unique physical properties.

Acknowledgements

This work is supported by the New Energy and Industrial Technology Development Organization (NEDO) for the ‘Project on the Nanostructured Polymeric Materials’.

References

[1] Stein RS, Khambatta FB, Warner FP, Russell TP, Escala A, Balizer E. J Polym Sci, Polym Symp 1978;63:313.
[2] Chen HL, Wu SF, Lin TL, Wu GM. Polym J 2002;34:356.
[3] Vanneste M, Groeninckx G, Reynaers H. Polymer 1997;38:4407.
[4] Chen HL, Li LJ, Lin TL. Macromolecules 1998;31:2255.
[5] Talibuddin S, Wu L, Runt J, Lin JS. Macromolecules 1996;29:7527.
[6] Imken RL, Paul DR, Barlow JW. Polym Eng Sci 1976;9:593.
[7] Penning JP, Manley RSJ. Macromolecules 1996;29:77.
[8] Rahman MH, Nandi AK. Macromol Chem Phys 2002;203:653.
[9] Bernstein RE, Paul DR, Barlow JW. Polym Eng Sci 1978;18:1225.
[10] Becke RE, Cabasso I. Polymer 1988;29:1831.
[11] Lovinger AJ. In: Developments in crystalline polymers, vol. 1. London: Applied Science; 1981. p. P254.
[12] Nishi T, Wang TT. Macromolecules 1975;8:909.
[13] Morra BS, Stein RS. J Polym Sci, Polym Phys Ed 1982;20:2243.
[14] Roerdink E, Challa G. Polymer 1978;19:173.
[15] Saito H, Fujita Y, Inoue T. Polym J 1987;4:405.
[16] Roerdink E, Challa G. Polymer 1980;21:509.
[17] Morra BS, Stein RS. J Polym Sci, Polym Phys 1982;20:2261.
[18] Fatnassi M, Larbi FBC, Dubault A, Halary JL. e-Polymer 2005;1 [no. 056].
[19] Li YJ, Oono Y, Nakayama K, Shimizu H, Inoue T. Macromolecules, in revision.
[20] Fox TG. Bull Am Phys Soc 1956;2:123.
[21] Hsiao BS, Wang ZG, Yeh FJ, Gao Y, Sheth KC. Polymer 1999;40:3515.
[22] Verma R, Marand H, Hsiao B. Macromolecules 1996;29:7767.
[23] Jeong YG, Jo WH, Lee SC. Polymer 2003;44:3259.
[24] Woo EM, Wu MC. J Polym Sci, Polym Phys 2005;43:1662.
[25] Paul DR, Newman S. Polymer blend, Vol 1. New York: Academic Press; 1978.
[26] Gabriel OS, George PS. Polymer blends and alloys. New York: Marcel Dekker; 1999.
[27] Li YJ, Kaito A, Horiuchi S. Macromolecules 2004;37:2119.
[28] Li YJ, Kaito A. Macromol Rapid Commun 2003;24:255.
[29] Nishio Y, Yamane T, Takahashi T. J Macromol Sci, Phys 1984;B23:17.
[30] Ward IM. Structure and properties of oriented polymers. London: Chapman & Hall; 1997.